J. Biochem. 2011;150(2):157–163 doi:10.1093/jb/mvr046

JB THE JOURNAL OF BIOCHEMISTRY

A 68 residue N-terminal fragment of pro-atrial natriuretic peptide is a monomeric intrinsically unstructured protein

Received January 18, 2011; accepted March 25, 2011; published online April 20, 2011

Dan L. Crimmins[1,*] and Jeffrey L.-F. Kao[2]

[1]Department of Pathology and Immunology, Division of Laboratory and Genomic Medicine, Washington University School of Medicine, St Louis, MO 63110; and [2]Department of Chemistry, High Resolution NMR Facility, Washington University, St Louis, MO 63130, USA

*Dan L. Crimmins, Department of Pathology and Immunology, Division of Laboratory and Genomic Medicine, Washington University School of Medicine, St Louis, MO 63110, USA. Tel: +314 454 8514, Fax: 314-454-5208, email: crimmins@pathology.wustl.edu

The mature pro forms of the cardiac natriuretic peptides, atrial natriuretic peptide (ANP) and brain natriuretic peptide (BNP), are proteolytically processed to their active hormone forms (28 and 32 residues, respectively) and N-terminal (NT)-pro fragments (68 and 76 residues, respectively). Far-ultraviolet circular dichroism (UV CD), 1D and 2D-homonuclear nuclear magnetic resonance (NMR), size exclusion-high performance liquid chromatography (SE-HPLC) and analytical ultracentrifuge sedimentation equilibrium (AUCSE) data are obtained for NT-proANP. CD data showed a large negative molar ellipticity for NT-proANP of −14,800° cm^2/dmol at 199–200 nm. The intensity of the 1D-^{1}H NMR spectra in the amide region for NT-proANP was very low and confined to ~8–8.6 ppm. Furthermore, cross-correlation resonance peaks were absent in the corresponding 2D-^{1}H NOE spectra for NT-proANP in this region. The elution peak for this fragment from a G2000SW size-exclusion column was 20.4′; myoglobin (~17 K) was also eluted at 20.4′. No higher molecular weight oligomers were evident in the AUCSE experiments for NT-proANP. Collectively, the physical data demonstrate that NT-proANP, like NT-proBNP, is primarily a disordered, monomeric protein. Lastly, we compare the predictions from two *in silico* metaserver disorder algorithms, MeDor and MetaPrDOS, to the experimental data.

Keywords: atrial natriuretic peptide/intrinsically unstructured protein/monomer/natriuretic peptide/N-terminal atrial natriuretic peptide.

Abbreviations: ANP, atrial natriuretic peptide; AUCSE, analytical ultracentrifugation sedimentation equilibrium; BNP, brain natriuretic peptide; CD, circular dichroism; GdmCL, guanidine hydrochloride; HPLC, high performance liquid chromatography; NMR, nuclear magnetic resonance; NT, N-terminal; SE, size exclusion; NOE, nuclear Overhauser effect; UV, ultraviolet.

The cardiac natriuretic peptides, ANP and BNP, are hormones that regulate cardiovascular function (*1*). Each is synthesized as a preprohormone molecule and the mature prohormone form is further processed by proteolytic convertases into the active hormone and NT-pro fragments (*1*). Clinically, both BNP and NT-proBNP are widely used in an immunoassay format to assess left ventricle dysfunction (*2*). Even though ANP was discovered before BNP (*3*), it has not received as much attention, although recently a commercial immunoassay to mid-region proANP has been introduced (*4*). Moreover, the physicochemical properties and post-translational modifications of proBNP and NT-proBNP have been studied extensively (*5–8*).

Exogeneous NT-proBNP and proBNP have been shown to be monomeric proteins with little or no secondary structure (*5*, *6*). Glycosylation of specific S and T residues was identified in proBNP recombinant proteins expressed in CHO (*7*) and HEK293 (*6*) cell lines. In addition, a recent study found that recombinant protein expressed in either HEK293 or HL-1 cell lines was also O-glycosylated (*8*). Sera from heart failure patients were inferred to be O-glycosylated following glycosidase treatment and gel electrophoresis. Intriguingly, O-glycosylation near the convertase cleavage site inhibited processing such that heart failure patients had an unexpectedly high fraction of proBNP compared to BNP and NT-proBNP (*9*). It is reasonable to expect then that these studies will aid in the development of more specific and clinically informative immunodiagnostic assays of cardiac dysfunction (*10*).

In contrast to the above proBNP work, very little is known about the physical properties and post- and co-translational modification of proANP. In this report empirical and *in silico* data are presented on the secondary structure, and on the oligomeric state of a 68-residue NT-proANP in near neutral pH physiologic buffer at milligram per millilitre protein concentrations.

Materials and Methods

NT-proANP was annotated from accession number P01160 at the ExPASy Proteomics site http://us.expasy.org/. The 68-residue protein, EVVPPQVLSEPNEE AGAALSPLPEVPPWTGEVSPAQ RDGGALGRGPWDSSDRSALLKSKLRALLTAPR, was synthesized at Biomolecules Midwest, Inc. (Waterloo, IL, USA). The lyophilized sample was dissolved in and exhaustively dialysed versus PBS pH 7.2 containing 0.05% NaN_3. Protein concentration was estimated from $\varepsilon_{280} = 1.6$ (ml cm)/mg calculated at the ExPASy Proteomics Server. Detailed experimental conditions and analysis for far-UV CD, 1D and 2D-^{1}H homonuclear NMR, SE-HPLC and AUCSE have been described elsewhere (*5*, *6*, *11*). Proton T1

(spin–lattice) and T2 (spin–spin) relaxation time were measured by inversion recovery and CPMG methods (*12*), respectively. Proton spectral width was set to 7200 Hz with a 13.1 μs for 90° pulse and 26.2 μs for 180° pulse. Two *in silico* programs (*13*) were used to predict disorder, MeDOR (*14*) and metaPrDOS (*15*).

Results and Discussion

Far-UV CD

Unstructured proteins have a diagnostic large negative ellipticity in the 197–200 nm region with little of the other secondary structure elements (*e.g.* helix, sheets, turns) present in far-UV CD measurements (*16*, *17*). Figure 1 displays a room temperature CD spectrum for NT-proANP in a physiologic near neutral pH buffer. A minimum is observed at ~199–200 nm giving a value of −14,800° cm^2/dmol indicating that the 68-residue NT-proANP fragment is largely unstructured. For comparison, unstructured 76-residue NT-proBNP, another cardiac natriuretic peptide (*1*, *18*), has an ellipticity of −19,000° cm^2/dmol at ~198 nm (*5*, *6*, *11*). The lack of structure is simply not a consequence of the small size of each natriuretic peptide fragment because a 58-residue fragment of cholecystokinin (CCK-58) shows appreciable helix content (*19*) as assessed by similar CD measurements (*20*).

1D and 2D-homonuclear NMR

Figure 2B shows the 4°C proton spectra for NT-proANP in 10% D_2O. The intensity in the amide region is rather low and confined to a narrow region of ~8–8.6 ppm. In contrast, the NH resonances for known folded proteins such as bovine pancreatic trypsin inhibitor (BPTI, a 58-residue protein) are dispersed from ~7.5 to 10.2 ppm as illustrated in Fig. 2A (*21*). Moreover, it was found that the amide resonances disappeared immediately after the freshly prepared protein was dissolved in D_2O solution (Fig. 2D). This indicated that the amide protons are accessible to the solvent and the protein has no well-defined hydrogen bonds. T1 (spin–lattice) and T2 (spin–spin) relaxation time measurements on tryptophan resonance at 10.2 ppm are displayed in Fig. 3A and B, respectively. The observed 0.86 s T1 and 0.038 s T2 relaxation time measurements suggest the protein has correlation time in the 10^{-9} s range, which is typical for small protein such as NT-proANP and BPTI (*22*). It is difficult to obtain complete side chain and backbone resonances assignment without ^1H and ^{13}C isotopically labelling of the protein. The cross-correlation NH(i) − NH($i+1$) resonance peaks from homonuclear 2D-NOE are essentially absent (supplementary Fig. S1) indicating little overall solution structure for NT-proANP, a result also found for NT-proBNP (*11*). This is consistent with the result of the proton exchange experiment shown in Fig. 2C and D.

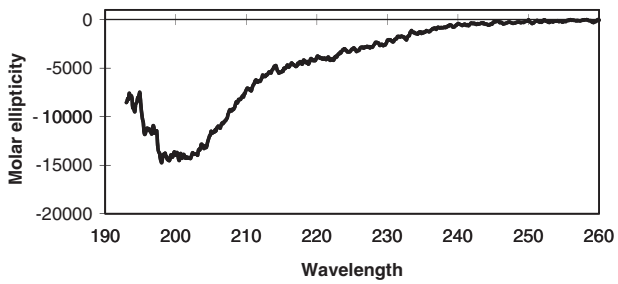

Fig. 1 Room temperature far-UV CD of NT-proANP in PBS, pH 7.2 containing 0.05% NaN_3. Protein concentration of 0.75 mg/ml. Five scans were averaged and subtracted from a buffer blank scanned under the same conditions.

SE-HPLC

The separation mechanism in non-denaturing media for SE-HPLC is determined by the shape of the three-dimensional structure of the molecules undergoing chromatography and 'not' their molecular weight as often stated (*23*). This misinterpretation for the SE elution of pro and NT-pro natriuretic peptides led to the hypothesis that each protein was an oligomer (*24*). We have previously shown that BNP fragments (NT-proBNP and O-glycosylated proBNP) elute aberrantly on SE-HPLC yet are not oligomers (*5*, *6*). Figure 4A and B display the elution profile monitored at 214 nm for a protein column performance mixture (*5*) and 18 μg of NT-proANP, respectively. The ~7 K ANP fragment is seen to elute at the same time as 17 K myoglobin and one might erroneously conclude that NT-proANP is a dimer or trimer based on this co-elution. As myoglobin is known to adopt a compact, folded three-dimensional structure (*25*), and as the above far-UV CD and NMR data demonstrate that NT-proANP is largely unstructured in physiologic near neutral pH non-denaturing buffer, it is evident that shape, *e.g.* R_s the Stoke's radius, and not molecular weight is the determining mechanistic factor in SE-HPLC. On the same column, unstructured monomeric NT-proBNP eluted at 20.6′ (data not shown).

Uversky describes a set of equations relating log(R_s) to molecular weight for SE-HPLC (*26*). For NT-proANP with molecular weight of ~7.1 kD the ranges for a native globular-like protein, a native unstructured random coil and a GdmCl denatured protein are: 13.5–16.2, 19.1–25.7 and 20.4–26.9 Å, respectively. Our CD and NMR data show very little structure for NT-proANP and imply a coil-like conformation. In 5.2 M GdmCl, NT-proANP elutes slightly ahead of the corresponding sample in non-denaturing buffer (Supplementary Fig. S2). In contrast, for several of the proteins in the column performance mixture, their elution in denaturing buffer drastically shifts closer to the void volume marker for this column, thyroglobulin. Thus, these proteins are unfolded compared to their respective globular-like native states. The ratio of sample elution to void volume elution in denaturing and non-denaturing solvent was 0.67 and 0.62, respectively, or a native coil to denatured structure ratio (0.62/0.67) of 0.93. The ranges for the corresponding R_s values are 19.1/20.4–25.7/26.9, *i.e.* 0.94–0.96. The agreement between the two methodologies is excellent.

AUCSE

Sedimentation equilibrium experiments provide useful information on the quaternary structure of proteins.

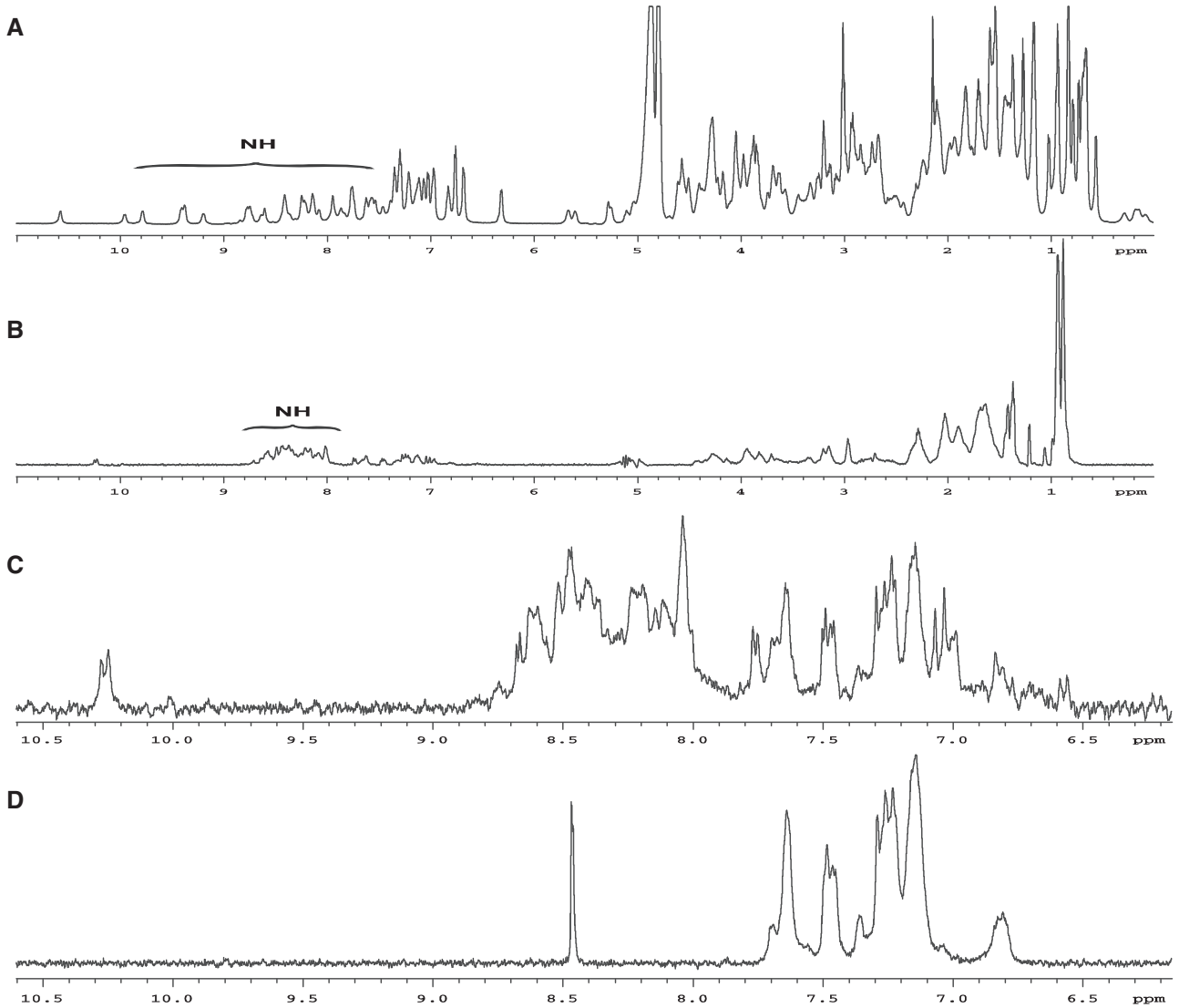

Fig. 2 NMR spectra of NT-proANP in PBS, pH 7.2 containing 0.05% NaN_3. Protein sample of 495 µl 3.6 mg/ml NT-proANP + 55 µl 99.994% D_2O; ~0.46 mM final. (A) 1D proton spectra at 4°C with the amide (NH) region indicated for BPTI and (B) for NT-proANP. (C) The 6.5 to 10.5 ppm region of Fig. 2b and (D) the same region for lyophilized NT-proANP resuspended in a D_2O solution.

This technique was used by us to demonstrate that at several protein concentrations and rotor speeds NT-proBNP, proBNP and O-glycosylated proBNP were monomers (*5*, *6*). We now show in Fig. 5 that NT-proANP joins this list. Here, for this 4°C run, the experimental value was found to be 7.2 K and is to be compared to the theoretical molecular weight of 7,126 for the unmodified 68-residue fragment. Note that this result makes it highly unlikely that the SE-HPLC elution profile of endogeneous proANP presented in (*24*) is due to oligomerization. Whether this aberrant elution behaviour can be ascribed to glycosylation or some other modification, as has been documented for BNP molecules (*7*), is not presently known. Interestingly, recombinant pro-ANP proteins expressed in HEK293 and HL-1 cells could not be shown to be O-glycosylated unlike proBNP molecules produced in the same cell lines (*8*).

In silico disorder algorithms

Two metaserver programs, MeDor and metaPrDOS, were used to predict disorder in NT-proANP (*13–15*). The idea behind these is to generate a consensus result from several individual disorder programs, and is thereby expected to improve the overall accuracy. Figure 6A and B present the results from these programs in a secondary structure representation along with the calculations from six individual algorithms (two of the programs 'timed-out'), and a consensus disorder frequency graph, respectively. In general, there is little secondary structure except for a predicted 4-turn helix from about S_{50} to L_{64} (Fig. 6A) and large overlap of predicted disordered regions. The metaPrDOS disorder plot (Fig. 6B), which is a consensus of different set of six individual programs, shows no residues below the default false-positive rate of 5%. Thus, all residues are classified as disordered by the

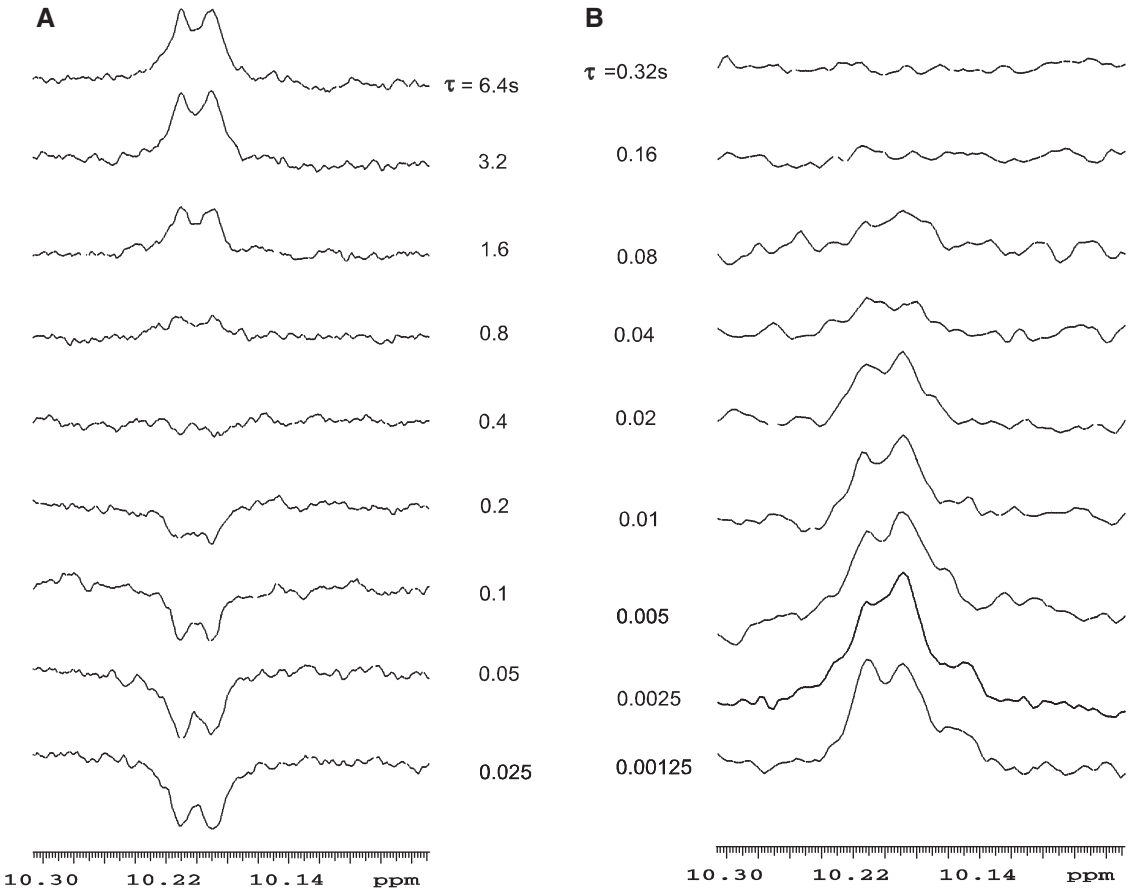

Fig. 3 T1 and T2 relaxation experiments at 4°C on the tryptophan NH resonances at 10.2 ppm for NT-proANP. (A) T1 and (B) T2 measurements.

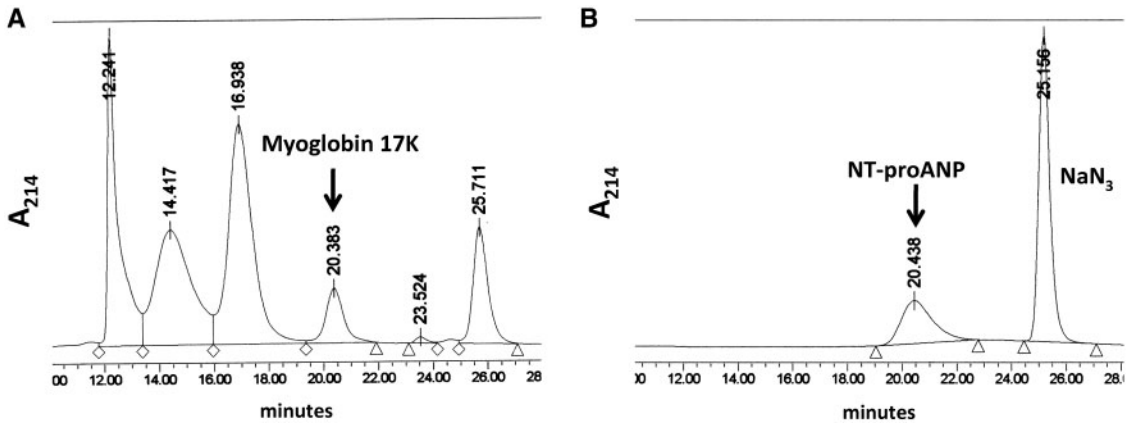

Fig. 4 Room temperature G2000SW SE-HPLC of NT-proANP. Flow rate of 1 ml/min in 50 mM sodium phosphate, 150 mM NaCl pH 6.5 on a 600 x 7.8 mm column. Elution monitored at 214 nm. (A) 10 µl of column performance mixture at 0.25 absorbance units full scale with elution position of myoglobin indicated and (B) 18 µg NT-proANP at 0.6 absorbance units full scale.

latter analysis. Collectively then, both metaserver algorithms predict very little order for NT-proANP. This observation is in good agreement with the empirical data described above and thus may bolster one's confidence in using this type of analysis as an aid in developing testable hypotheses. Indeed, a similar comparison for the 58 amino acid CCK-58 yields a helical stretch from G_7 to K_{26} using the secondary structure prediction program from MeDor and an ordered region from L_{13} to R_{25} using metaPrDOS (data not shown) in qualitative agreement with the CD data (*20*).

Conclusion

We have shown from the physicochemical measurements that the 68-residue NT portion of ANP is a monomeric intrinsically unstructured protein, a classification shared with another cardiac natriuretic

peptide NT fragment and proBNP. In addition, the calculations from the *in silico* algorithms were in general accord with this result. Why these domains of the cardiac natriuretic peptides are largely disordered and how that may contribute to cardiac homeostasis is not presently know. It is intriguing that each large NT fragment of proANP and proBNP, which are primarily expressed in different cardiac chambers, is mainly unordered. Two recent reviews (*27*, *28*) have tabulated a myriad of different functions for intrinsically disordered regions in proteins. Perhaps in the case of the two cardiac NP's described herein, the function of this plasticity is to facilitate or at least not impede processing by the convertases furin and corin (*29*). In this aspect, cell-based proteolysis experiments with chimera prohormones such as the NT-proANP fragment fused to BNP hormone and the converse, NT-proBNP fragment fused to proANP hormone may provide further insight into the function of these disordered regions. An earlier study did address the processing of prohormone precursor proteins at and near the cleavage site (*30*), but did not elucidate possible influences of the larger NT fragments. It will be interesting to see if biophysical measurements on the NT fragment of a non-cardiac third human natriuretic peptide: proCNP (*31*) also shows lack of order. In this regard, our preliminary *in silico* calculations on NT-proCNP (D.L. Crimmins and J.P. Goetze unpublished results) indicate little secondary structure, suggesting that NT fragment disorder may play a similar role for all three NT fragments by assuring a high fidelity of cleavage thus generating the active NP hormone. From a clinical

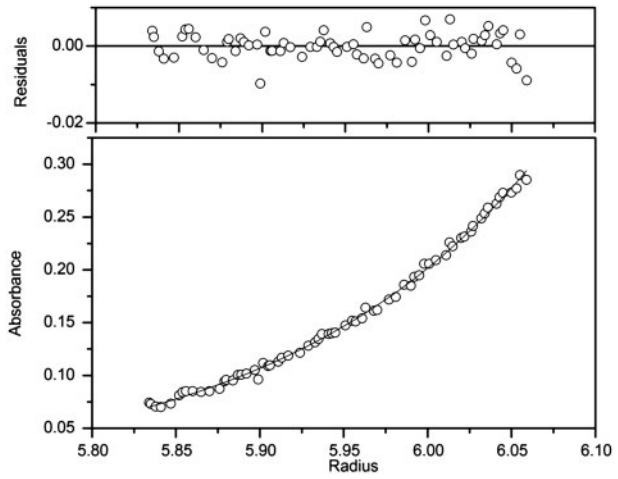

Fig. 5 AUCSE of NT-proANP in PBS, pH 7.2 containing 0.05% NaN_3. Protein concentration of 0.12 mg/ml with a rotor speed of 34 K rpm at 4°C. A single, ideal species model using XL-A/XL-I version 6.03 software based on software from Origin Labs Software, Inc. (Northhampton, MA, USA) was used to fit the data (*6*). This particular run gave a molecular weight of 7.2 K. Three different concentrations and 2 rotor speeds gave an average molecular weight of 7.4 K ± 1.4 K (SD, $n = 6$).

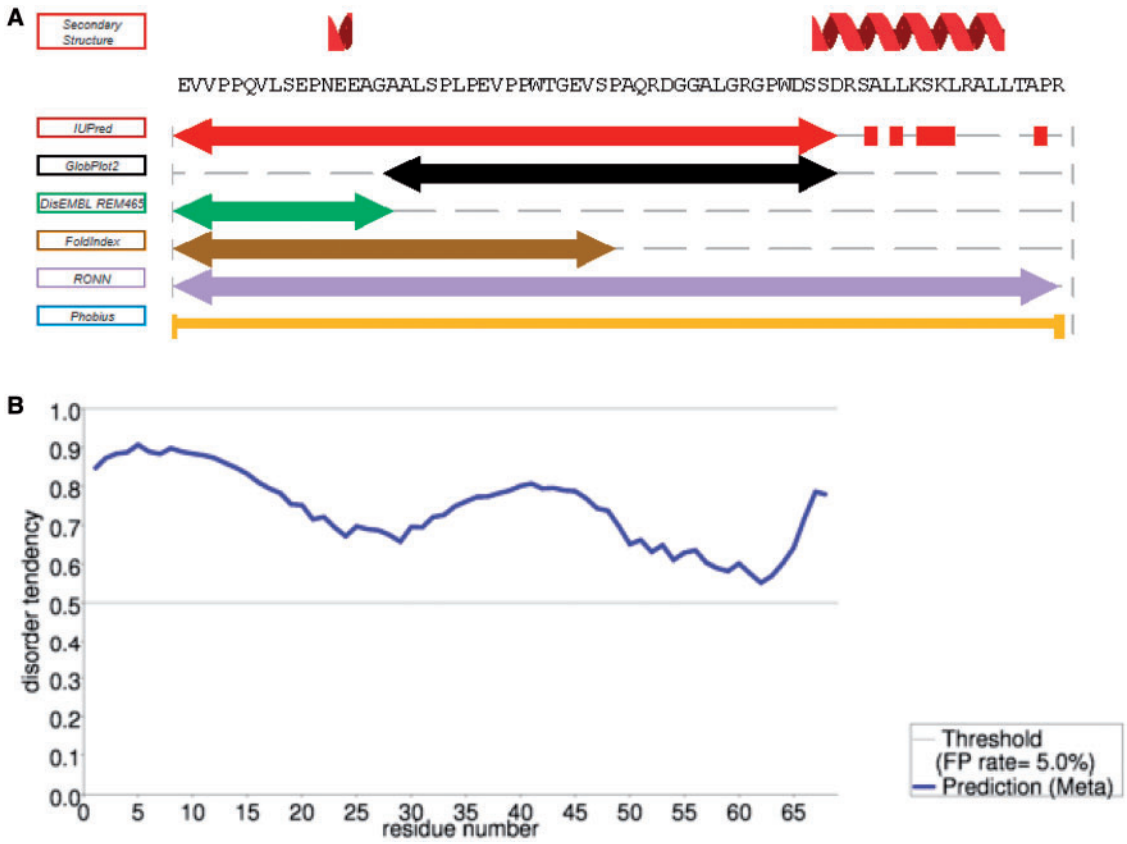

Fig. 6 *In silico* metaserver disorder algorithms applied to NT-proANP. (A) MeDor analysis generating a secondary structure plot and disordered regions from each of six individual programs and (B) metaPrDOS analysis generating a consensus disorder frequency plot from a different set of six individual programs.

perspective (*10*), sera from heart failure patients contain a larger than expected fraction of uncleaved proBNP (*9*). This phenomenon has been attributed to specific O-glycosylation near the cleavage site and whether a similar result will be found for proANP remains to be determined.

Supplementary Data

Supplementary Data are available at *JB* Online.

Acknowledgements

The authors thank Dr Jonathan Chaires (director) and Dr Nichola Garbett (co-director) of the Biophysics Service Center at Brown Cancer Centre at the University of Louisville for AUCSE studies. Portions of this work were presented at the 31st European Peptide Symposium in Copenhagen, Denmark September 2010.

Funding

Siemens Healthcare Diagnostics and the Department of Pathology and Immunology (to D.L.C., partial).

Conflict of interest

None declared.

References

1. Gardner, D.G., Kovaic-Milivojevic, B., Liang, F., and Chen, S. (1999) Hormones and the heart in *Health and Disease* (Share, L., ed.), pp. 1–20, Humana Press, Totowa, NJ
2. Luckenbill, K.N., Christenson, R.H., Jaffe, A.S., Mair, J., Ordonez-Llanos, J., Pagani, F., Tate, J., Wu, A.H.B., Ler, R., and Apple, F.S. (2008) Cross-reactivity of bnp, nt-probnp, and probnp in commercial bnp and nt-probnp assays: Preliminary observations from the IFCC committee for standardization of markers of cardiac damage. *Clin. Chem.* **54**, 619–621
3. deBold, A.J., Borenstein, H.B., Veress, A.T., and Sonnenberg, H. (1981) A rapid and potent natriuretic response to intravenous injection of atrial myocardial extract in rats. *Life Sci.* **28**, 89–94
4. Chenevier-Gobeaux, C., Guerin, S., André, S., Ray, P., Cynober, L., Gestin, S., Pourriat, J.-L., and Claessens, Y.-E. (2010) Midregional pro–atrial natriuretic peptide for the diagnosis of cardiac-related dyspnea according to renal function in the emergency department: A comparison with b-type natriuretic peptide (bnp) and n-terminal probnp. *Clin. Chem.* **56**, 1708–1717
5. Crimmins, D.L. (2005) Human n-terminal probnp is a monomer. *Clin. Chem.* **51**, 1035–1038
6. Crimmins, D.L. and Kao, J.L.-F. (2008) A glycosylated form of the human cardiac hormone pro b-type natriuretic peptide is an intrinsically unstructured monomeric protein. *Arch. Biochem. Biophys.* **475**, 36–41
7. Schellenberger, U., O'Rear, J.O., Guzzetta, A., Jue, R.A., Protter, A.A., and Pollitt, N.S. (2006) The precursor to b-type natriuretic peptide is an o-linked glycoprotein. *Arch. Biochem. Biophys.* **451**, 160–166
8. Jiang, J., Pristera, N., Wang, W., Zhang, X., and Wu, Q. (2010) Effect of sialylated *o*-glycans in pro–brain natriuretic peptide stability. *Clin. Chem.* **56**, 959–966
9. Semenov, A.G., Postnikov, A.B., Tamm, N.N., Seferian, K.R., Karpova, N.S., Bloshchitsyna, M.N., Koshkina, E.V., Krasnoselsky, M.I., Serebryanaya, D.V., and Katruka, A.G. (2009) Processing of pro–brain natriuretic peptide is suppressed by o-glycosylation in the region close to the cleavage site. *Clin. Chem.* **55**, 489–498
10. Mair, J. (2009) Clinical significance of pro-b-type natriuretic peptide glycosylation and processing. *Clin. Chem.* **55**, 394–397
11. Crimmins, D.L. and Kao, J.L.-F. (2007) The human cardiac hormone fragment n-terminal pro b-type natriuretic peptide is an intrinsically unstructured protein. *Arch. Biochem. Biophys.* **461**, 242–246
12. Carr, H. and Purcell, E. (1954) Effects of diffusion on free precession in nuclear magnetic resonance experiments. *Phys. Rev.* **94**, 630–638
13. Tompa, P. (2010) Prediction of disorder in *Structure and Function of Intrinsically Disordered Proteins* (Tompa, P., ed.), pp. 103–114, CRC Press, Boca Raton, FL
14. Lieutaud, P., Canard, B., and Longhi, S. (2008) MeDor: a metaserver for predicting protein disorder. *BMC Genomics* **9 (Suppl. 2)**, S25
15. Ishida, T. and Kinoshita, K. (2008) Prediction of disordered regions in proteins based on the meta approach. *Bioinformatics* **24**, 1344–1348
16. Tompa, P. (2010) Spectroscopic techniques for characterizing disorder in *Structure and Function of Intrinsically Disordered Proteins* (Tompa, P., ed.), pp. 63–65, CRC Press, Boca Raton, FL
17. Woody, R.W. (2010) Circular dichroism of intrinsically disordered proteins in *Instrumental Analysis of Intrinsically Disordered Proteins* (Uversky, V.N. and Longhi, S., eds.), pp. 303–322, Wiley, Hoboken, NJ
18. Goetze, J.P. (2009) Biosynthesis of cardiac natriuretic peptides. Results Probl. *Cell Differ.* **25**, 97–120
19. Greenfield, N. and Fasman, G.D. (1969) Computed circular dichroism spectra for the evaluation of protein conformation. *Biochemistry* **8**, 4108–4116
20. Keire, D.A., Solomon, T.E., and Reeve, J.R. Jr (1999) Identical primary sequence but different conformations of the bioactive regions of canine cck-8 and cck-58. *Biochem. Biophys. Res. Commun.* **266**, 400–404
21. Wagner, G. and Wuthrich, K. (1982) Sequential resonance assignments in protein ^{1}H nuclear magnetic resonance spectra: Basic pancreatic trypsin inhibitor. *J. Mol. Biol.* **155**, 347–366
22. Ishima, R., Shibata, S., and Akasaka, J. (1995) General features of proton longitudinal relaxation in proteins in solution. *J. Magn. Reson.* **91**, 455–465
23. Gooding, K.M. and Regnier, F.E. (1990) Size exclusion chromatography in *HPLC of Biological Macromolecules* (Gooding, K.M. and Regnier, F.E., eds.), pp. 47–75, Marcel Dekker, New York, NY
24. Seilder, T., Pemberton, C., Yandle, T., Espiner, E., Nicholls, G., and Richards, M. (1999) The amino terminal regions of probnp and proanp oligomerise through leucine zipper-like coiled-coil motifs. *Biochem. Biophys. Res. Commun.* **255**, 495–501
25. Kendrew, J.C., Bodo, G., Dintzis, H.M., Parrish, R.G., Wyckoff, H., and Phillips, D.C. (1958) Three-dimensional model of the myoglobin molecule obtained by X-ray analysis. *Nature* **181**, 662–666
26. Uversky, V.N. (2010) Analyzing intrinsically disordered proteins by size exclusion chromatography in *Instrumental Analysis of Intrinsically Disordered Proteins* (Uversky, V.N. and Longhi, S., eds.), pp. 525–544, Wiley, Hoboken, NJ
27. Turoverov, K.K., Kuznetsova, I.M., and Uversky, V.N. (2010) The protein kingdom extended: Ordered and intrinsically disordered proteins, their folding, supramolecular complex formation, and aggregation. *Prog. Biophys. Mol. Biol.* **102**, 73–84

28. Uversky, V.N. and Dunker, A.K. (2010) Understanding protein non-folding. *Biochim. Biophys. Acta* **1804**, 1231–1264
29. Semenov, A.G., Tamm, N.N., Seferian, K.R., Postnikov, A.B., Karpova, N.S., Serebryanaya, D.V., Koshkina, E.V., Krasnoselsky, M.I., and Katrukha, A.G. (2010) Processing of pro–b-type natriuretic peptide: Furin and corin as candidate convertases. *Clin. Chem.* **56**, 1166–1176
30. Harris, R.B. (1989) Processing of pro-hormone precursor proteins. *Arch. Biochem. Biophys.* **275**, 315–333
31. Lippert, S.K., Rehfeld, J.F., and Goetze, J.P. (2010) Processing-independent analysis for pro-c-type natriuretic peptide. *J. Immunol. Methods* **362**, 32–37